Natural Hazards (2022) 113:213–236
https://doi.org/10.1007/s11069-022-05296-w

ORIGINAL PAPER

Detection, characterization, and analysis of land subsidence in Nairobi using InSAR

Pius Kirui[1,3] · Samson Oiro[2] · Hunja Waithaka[3] · Patroba Odera[4] · Björn Riedel[1] · Markus Gerke[1]

Received: 6 July 2021 / Accepted: 17 February 2022 / Published online: 31 March 2022

Abstract

Nairobi, Kenya's capital city, is one of the fastest-growing cities on the continent. The rapid expansion of human activities has resulted in the overexploitation of natural resources, such as water. In the past, Nairobi had been identified as a vulnerable area to environmental hazards, such as land subsidence. Due to the lack of a functioning deformation-monitoring system in Kenya, the subsidence in Nairobi has yet to be empirically quantified. In this paper, we report the results of the first InSAR-based spatial assessment of land subsidence in Nairobi. Our analysis indicates both localized and regionalized subsidence in several locations in the west and north west of Nairobi. The largest deforming unit in Nairobi's western part is subsiding at approximately 62 mm/yr. Land subsidence can be attributed to groundwater overexploitation because it coincides with regions with the highest decline in groundwater levels. However, subsidence can also be attributed to consolidation associated with rapid urbanization in other areas such as east of Nairobi. This evaluation corroborates previous hydrogeological investigations which indicated that Nairobi was at risk of subsidence, contributing to flooding in some residential areas. The findings will help guide future decision-making in several agencies as well as provide an effective tool for planning mitigation measures to prevent further subsidence. A few of these include regulating borehole drilling, planning of roads and buildings, and locating groundwater observation wells. In addition, the observed significant land subsidence stresses the need for an updated geodetic reference system. Since Nairobi plays a significant role in the economy of Kenya, the effects of subsidence may be devastating and it is imperative that steps are taken to minimize their impact.

Keywords Nairobi land subsidence · Nairobi groundwater · Sentinel-1 · InSAR · Depletion of Nairobi aquifer

✉ Pius Kirui
p.kirui@tu-braunschweig.de

[1] Institute of Geodesy and Photogrammetry, Bienroder weg 81, 38106 Braunschweig, Germany

[2] Water Resources Authority, Nairobi, Kenya

[3] Department of Geomatic Engineering and Geospatial Information Systems, Jomo Kenyatta University of Agriculture and Technology, Nairobi, Kenya

[4] Division of Geomatics, School of Architecture, Planning and Geomatics, University of Cape Town, Cape Town, South Africa

1 Introduction

Land subsidence is a geohazard that can affect both rural and urban areas. Human activities make it particularly intense in urban areas, and its occurrence has been documented in several cities around the world (Motagh et al. 2017). Overexploitation of groundwater has resulted in land subsidence in cities such as Mexico (Chaussard et al. 2014), China (Chen et al. 2003), Italy (Ezquerro et al. 2020), Nepal (Bhattarai et al. 2017), Indonesia (Abidin et al. 2011), and Brazil (de Luna et al. 2017). There is also evidence that other human activities, such as rapid urbanization (Pratesi et al. 2016; Yang et al. 2018), consolidation of buildings and landfills (Chen et al. 2015; Mwau 2019; Baek et al. 2019), and changes in land use can also accelerate the subsidence process. Globally, the interaction between these human activities makes cities that are rapidly growing more vulnerable to subsidence.

Nairobi City, the capital city of Kenya, is among the fastest-growing cities in Africa (Ren et al. 2020). Nairobi's population is estimated at 4.3 million according to the 2019 Kenya National Bureau of Statistics (KNBS 2019), representing an increase of approximately 250 percent over the last three decades. The city hosts a variety of land uses, including residential, industrial, transportation, and commercial. In recent decades, population growth has put pressure on existing resources, creating environmental problems such as pollution, flooding, and shortages of basic necessities such as housing and water. Consequently, housing demand has increased, resulting in the construction of high-rise buildings and shopping malls, as well as other infrastructure projects (Otiso and Owusu 2008). In response to the increase in population and rapid urbanization, groundwater is being overexploited to meet the demand for residential, commercial, and industrial activities (Mumma et al. 2011; Chakava et al. 2014).

The Nairobi Water Sewerage Company, the agency responsible for Nairobi's water supply, provides 525,000 m^3 of water every day in contrast with Nairobi's daily water demand of 790,000 m^3 (NWSC 2019). Because of the unreliability of piped water, most residential houses and other establishments rely on groundwater for their water needs. Oiro et al. (2020) argues that groundwater extraction has increased in proportion to population growth and has resulted in aquifer depletion. The depletion of an aquifer is marked by a decrease in the water table, which occurs at a rate of 3-7m per year in Nairobi City. Subsequently, a reduction in groundwater table can cause land subsidence. Subsidence due to groundwater exploitation is caused by effective stress distribution in the strata, as well as compression of aquifers (Guo et al. 2015). A number of previous hydrogeological studies, including those conducted by Foster and Tuinhof (2005), Nairobi City Council (2007), and Onyancha et al. (2012) suggested that overexploitation of groundwater may have caused land subsidence in Nairobi.

To meet the increasing demand for housing, Nairobi has seen the rapid construction of high-rise buildings in areas that were not zoned for such structures (Makunda 2018; Mwaura and Odera 2021). As in other cities, rapid development of buildings can also cause land subsidence as a result of consolidation. Also, unplanned development in vulnerable ecological locations, such as floodplains where high populations reside, could lead to subsidence (Rateb and Abotalib 2020). Added to that, the exponential increase in waste and no alternative disposal sites for waste have put pressure on the existing landfill, the Dandora landfill, where 5000 tons of garbage are disposed every day (Hudson Hill 2020; Haregu et al. 2017). Apart from obvious environmental hazards, the daily addition of such amount of waste is a recipe for land subsidence caused by mechanical and biochemical processes at the landfill (Gasperini et al. 2014; Baek et al. 2019). Land subsidence could be

triggered by the interplay between these factors and aquifer depletion. In light of the risk factors mentioned above, monitoring land subsidence is essential to avoid losses such as the destruction of properties due to land subsidence.

A first effort at modeling land subsidence in Nairobi was made in 2014 by Mathu et al. (2014), who estimated a maximum of 5.9 m of subsidence over 80 years. The authors noted that no land subsidence associated with groundwater extraction had ever been reported in Nairobi because there is no deformation monitoring framework. Moreover, they based their calculations on hydrogeological and piezometric data. These estimates were cumulative, not spatially represented, and limited to observation wells with temporal data. The spatial representation of land subsidence has yet to be reported or quantified directly.

There have been numerous geodetic methods used to quantify land subsidence magnitude, including leveling (Chrzanowski et al. 1989; Tosi et al. 2007), Global Navigation Satellite Systems (GNSS) (Ustun et al. 2010; Argyrakis et al. 2020) and interferometric synthetic aperture radar (InSAR) (Chaussard et al. 2014; Hirose et al. 2001). While leveling and GNSS display point deformations with the highest accuracy, setting up and maintaining the networks is more costly. Maintenance and observation of Kenya's geodetic network is the responsibility of the national mapping agency, Survey of Kenya (SOK). Unfortunately, geodetic networks are not modern and up-to-date for mapping and other applications such as geophysical studies. The leveling geodetic network has not been updated or enhanced over the years, which means that deformation monitoring is impossible based on historic data. Additionally, Kenya lacked a reliable GNSS network, except for three stations owned by the International GNSS Service (IGS). A few efforts have recently been made by the private sector, such as Measurement Systems Limited, to establish a private geodetic network and a deformation monitoring network, such as the Uganda-Kenya Eastern Branch GNSS Network (Stamps et al. 2019). Due to the small size and sparse coverage of the network in Nairobi City County, the study area, its applicability in deformation monitoring is limited. It is possible that the lack of previous studies on deformation is due to the lack of accurate and adequate geodetic information in the study area.

InSAR's ability to monitor large spatial extents makes it well suited for monitoring land subsidence (Guo et al. 2015; Neelmeijer et al. 2018). Increased use of InSAR for deformation monitoring can be attributed to data availability from satellite missions such as the European Space Agency (ESA) Sentinel-1, along with improvements in processing algorithms implemented in open-source software platforms. Moreover, InSAR has the advantage of providing other auxiliary information such as damage to structures, profiling of aquifer systems, and the influence of geological structures on land subsidence (Motagh et al. 2017; Haghighi and Motagh 2019). Differential InSAR has previously been used to study subsidence, but errors such as decorrelation and tropospheric delay affected the ability to extract deformation signals or rendered them unreliable. The development of multitemporal InSAR (MTI) addressed these challenges, resulting in improved accuracy of the InSAR-derived measurements (Ferretti et al. 2000; Berardino et al. 2002). Typically, InSAR measurements are taken along the line of sight (LOS); however, using data collected in ascending and descending orbits, vertical and east-west components can be calculated (Hu et al. 2014; Eriksen et al. 2017).

Hence, this study aims to determine and characterize the nature of land deformation within Nairobi City County through InSAR by leveraging the large Sentinel-1 and ALOS data sets. The LOS velocity estimates are decomposed into vertical and east-west movements using data from ascending and descending orbits. In addition, we examine the possible causes of subsidence in Nairobi, such as overexploitation of groundwater and rapid urbanization.

2 Materials and methods

2.1 Study area

The study is conducted in Nairobi City County, Kenya's capital. Figure 1 illustrates the geographic extent, elevation, the processing extents limited to the footprint of the ascending orbit, and the geology.

The proximity of Nairobi to the Rift Valley has influenced its geomorphology owing to volcanic activity in the Rift (Onyango 2018). Nairobi's geological structure

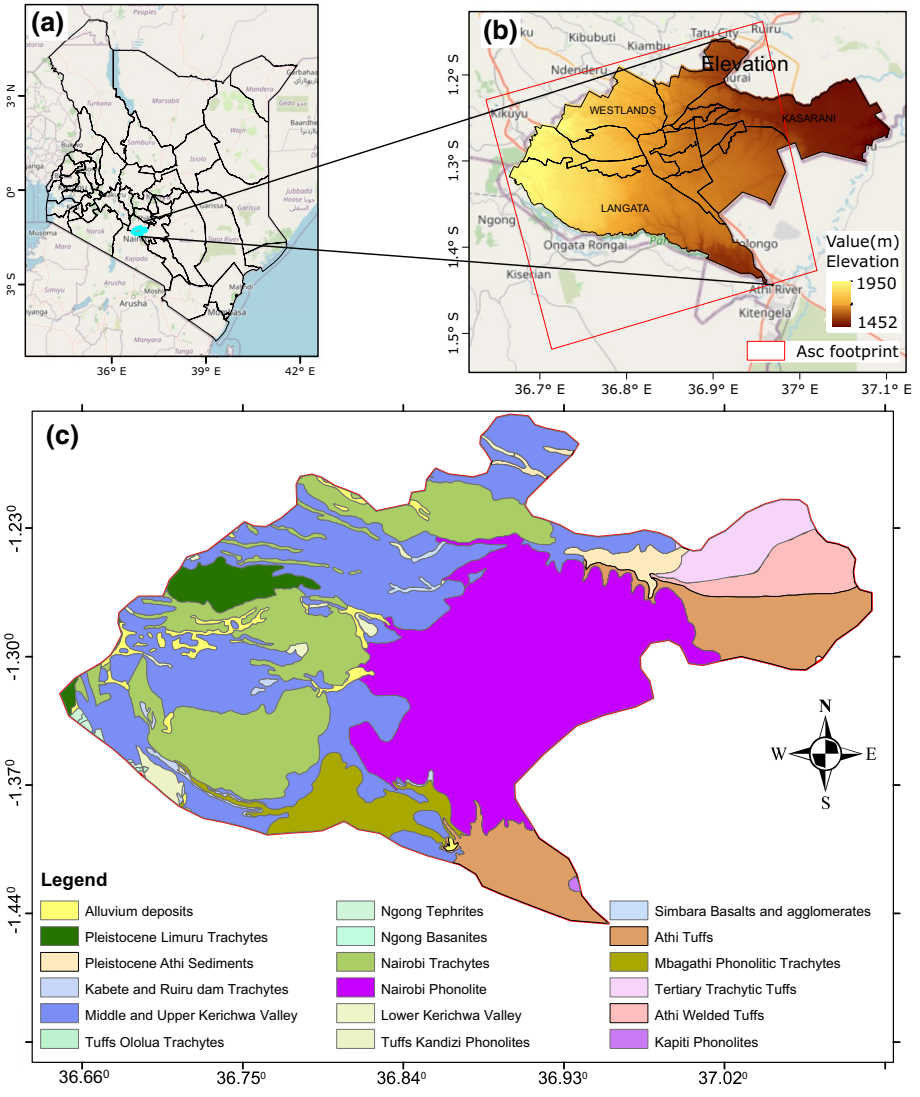

Fig. 1 The location of the study area (**a**). (**b**) shows the elevation of the site and the footprint of Sentinel-1's ascending orbit, while (**c**) shows the geology of the site

is dominated by pyroclastic volcanic rocks and sediments deposited in a series of lakes that stretch from Doinyo Sabuk to Kajiado (Matheson 1966; Onyancha et al. 2011). In Nairobi, the major geological structures are Nairobi trachyte to the west and northeast, Nairobi phonolite and Trachytic tuff to the east, and Kerichwa tuffs covering the northern and central parts of Nairobi. In addition, Mbaghati and Athi tuffs can be found to the southeast and Limuru tuffs to the northwest of Nairobi (Guth and Wood 2013). Nairobi's drainage system and groundwater are influenced by these geological formations. Because of their porosity, Nairobi's western and northern geological formations are more conducive to the occurrence of groundwater than its eastern formations, which are substantially impermeable. Due to faulting and weathering of former land surfaces and high rainfall coupled with groundwater recharge, groundwater flows southeast from west of Nairobi (Foster and Tuinhof 2005). Geological formations with different permeability rates have created multilayer aquifer systems, whose thickness increases westward of the exposed Athi tuffs. Rapid and significant localized aquifer depletion within Nairobi County is associated with a high abstraction rate due to high demand for water for residential and commercial use, as well as rapid urbanization, which alters the aquifer recharge system (Oiro et al. 2020).

2.2 Data

2.2.1 Sentinel-1 data

Sentinel-1 C-band data from the European Space Agency (ESA) were used in this study. Sentinel-1 A was launched in April 2014, but its initial observations in the study area were marred by gaps that rendered them unsuitable for multitemporal InSAR analysis. The launch of Sentinel-1 B in April 2016 enabled consistent observations to be made. As a result, the observations were consistent and the revisit time from beginning of 2017 to date was reduced from 24 days to 12 days. The Sentinel-1 data are acquired in interferometric wide (IW) mode, and each image consists of three sub-swaths that can act independently. The IW is imaged through the ScanSAR mode called Terrain Observation with Progressive Scan (TOPS) to improve the uniform signal-to-noise ratio (SNR). The product is distributed with a swath of 250 km and a resolution of 5×20 in range and azimuth, respectively (Geudtner et al. 2014). A total of 127 Sentinel-1 images are available for our study area, covering frame 1178 from ascending orbit path 130 and 99 images from descending orbit path 79 covering frame 597. The data is downloaded from the Alaska satellite facility Distributed Active Archive Data (ASF DAAC).

2.2.2 ALOS PALSAR 1

The Advanced Land Observing Satellite(ALOS), the PALSAR L-band SAR was launched in May 2006 and operated until 2011 by the Japan Aerospace Exploration Agency (JAXA). In the study area, 13 images are available from July 2007 to October 2010. We downloaded both the single polarization (FBS) and dual-polarization (FBD) formats acquired in ascending mode along path 566 with spatial resolution of 10 m and 20 m, respectively. The data were downloaded from the ESA ALOS PALSAR Dissemination Service in a raw format.

2.2.3 Groundwater data

Groundwater data for Nairobi County is obtained from the Water Resources Authority (WRA). WRA is charged with managing and regulating Kenya's water resources. They are responsible for issuing permits for the extraction of groundwater. Nairobi city has been categorized as part of the Nairobi aquifer system (NAS). We extracted data from the NAS borehole database to obtain groundwater information in the study area. Figure 2 shows Nairobi's boreholes' spatial distribution and temporal evolution.

In total, 1185 boreholes were found in the study area and the data cover the period from 1930 to 2018. In light of illegal borehole drilling and lack of a comprehensive borehole database, the number of boreholes presented here is an underestimation of the actual number of boreholes. Nairobi has an unknown number of boreholes, with different studies reporting different numbers (Nato 2015). As an example, Chakava et al. (2014) reports that in 2011, the WRA conducted surveys which indicated that there were 2139 boreholes, which is deemed a gross underestimation according to the researchers. According to Oiro et al. (2020), the number of boreholes is more than 5000 based on the number of applications received by WRA at the Nairobi sub-region office on average per day, not including illegal borehole drilling. While the exact number of boreholes is unknown, previous studies have found that the number of boreholes has increased exponentially over the last two decades. This is indicated by a decrease in the water table.

2.3 InSAR processing

2.3.1 Sentinel-1 processing

The InSAR Scientific Computing Environment (ISCE) is used to generate a stack of focused Single look complex (SLC) images. Coregistration is carried out following the network-based enhanced spectral diversity (NESD) approach (Fattahi et al. 2016). NESD ensures a higher accuracy in coregistration required for images acquired in TOPS mode to avoid phase discontinuities (Prats-Iraola et al. 2012). We process the coregistered SLC stack to generate the interferograms required for multi-temporal processing. In order to create a robust and interconnected network, we chose interferometric pairs with a maximum geometric baseline of 300 meters and a maximum temporal baseline of 48 days. The SBAS network used in this study is shown in Appendix A. For MTI, we use the modified SBAS (Hooper et al. 2012) implemented in the Stanford Method for Persistent Scatterers/Multi-Temporal InSAR (StaMPS/MTI) package. It works on single-look complex interferograms to select slowly decorrelating filtered phase pixels instead of the multi-looked interferograms as implemented in the conventional SBAS (Berardino et al. 2002). The permanent scatterers (PS) are initially selected based on the amplitude dispersion difference $D_{\Delta,A}$ (Hooper 2008) which is defined as,

$$D_{\Delta,A} = \frac{\sqrt{\frac{\sum_{i=1}^{N}(|m_i|-|s_i|)^2}{N}}}{\frac{1}{2N}\sum_{i=1}^{N}|s_i|} = \frac{\delta_{\Delta,A}}{\mu_{\Delta,A}} \tag{1}$$

where N is the number of images, S_i and M_i are the amplitudes of the slave and master, respectively, such that $\delta_{\Delta,A}$ is the standard deviation of the difference in amplitude between the master and slave; and $\mu_{\Delta,A}$ is the mean amplitude. All scatterers with an amplitude dispersion difference of less than 0.4 are initially selected as potential permanent scatterers.

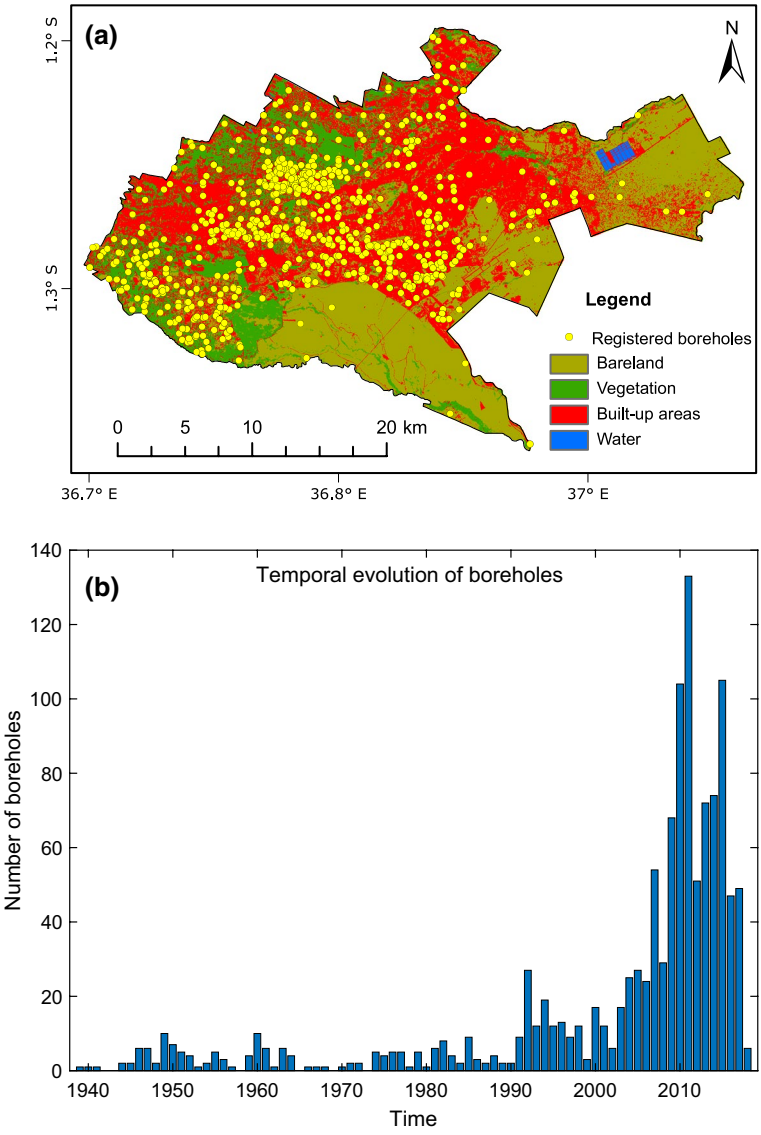

Fig. 2 The spatial distribution and the temporal evolution of boreholes in Nairobi County. (**a**) shows the spatial distribution of boreholes in relation to the land cover map, whereas (**b**) shows the temporal evolution of boreholes from 1930 to 2018

The final selection of PS candidates is determined by the phase stability based on the temporal coherence of the selected scatterers, which is expressed as,

$$\gamma_x = \frac{1}{N} \left| \sum_{i=1}^{N} \exp \sqrt{-1} (\psi_{x,1} - \tilde{\psi_{x,1}} - \Delta\tilde{\phi}_{\theta,x,i}) \right| \tag{2}$$

where $\psi_{x,1}$ is the wrapped phase, $\tilde{\psi_{x,1}}$ is the spatially uncorrelated term and $\Delta\tilde{\phi}_{\theta,x,i}$ is the spatially correlated term. The spatially correlated components in the interferograms are estimated by bandpass filtering in the frequency domain. The spatially uncorrelated look angle error is subtracted based on its correlation with the geometric baseline. Subtraction leaves spatially correlated terms including decorrelation noise, deformation, and atmospheric noise. The interferograms corrected for spatially uncorrelated errors are unwrapped using the 3D minimum cost flow function unwrapping algorithm (Hooper and Zebker 2007). The tropospheric delay is estimated through time series filtering by applying a low-pass spatial filter and a high-pass temporal filter. MTI processing is perfomed for both the ascending and ascending data. The velocity estimates from both orbits are combined to estimate the vertical and east-west components. The velocity estimates are first interpolated into a regular grid to ensure that pixels are present in both tracks and cover similar spatial extents. The vertical and east-west components are determined using Eq. 3. We do not estimate the north-south component because of the low sensitivity of InSAR measurements in the north-south direction.

$$\begin{bmatrix} \cos\theta_{asc} & -\sin\theta_{asc}\cos\alpha_{asc} \\ \cos\theta_{dsc} & -\sin\theta_{dsc}\cos\alpha_{dsc} \end{bmatrix} \begin{bmatrix} d_v \\ d_E \end{bmatrix} = \begin{bmatrix} d_{los_a sc} \\ d_{los_d sc} \end{bmatrix} \tag{3}$$

where θ is the incidence angle, α is the heading angle of the satellite, d_v is the movement in the vertical direction, and d_E is the movement in the horizontal direction. We use the incidence angle at each pixel's location to determine the vertical and horizontal components owing to the varying nature of the Sentinel-1 incidence angle.

2.3.2 ALOS InSAR processing

We used ENVI SARscape (Sahraoui et al. 2006) to convert the raw co-polarized FBS and FBD ALOS Palsar data into single-look complex images and to perform SBAS MTI processing. The SLC images are used to construct a small baseline network with a geometric baseline of 1728 m and a temporal baseline of 736 days, ensuring that all the images are connected in the network, as shown in Appendix B. Although our data consists of a few images, the condition is achieved given that the L-band data are least affected by geometric decorrelation owing to their longer baselines (Sandwell et al. 2008). Moreover, our study area is mainly covered by built-up areas that guarantee good coherence even for longer temporal baselines. Multi-look interferograms are generated and filtered using the Goldstein filter (Goldstein and Werner 1998) to increase the signal-to-noise ratio and are unwrapped using the minimum cost flow (MCF) algorithm. The 90 m Shuttle Radar Topography Mission (SRTM) DEM is used to remove the topographic influence. The interferograms are then refined to remove orbital errors through polynomial fitting of degree three using ground control points. Atmospheric noise is estimated and accounted for through time-series filtering by applying a low-pass filter in space and a high-pass filter in time. The unwrapped phases corrected for atmospheric delay were inverted to estimate the velocity and time series displacement, assuming that the displacement is in a vertical direction based on the results of the Sentinel-1 analysis.

2.4 Borehole data processing

A time-series analysis of the borehole data is performed to determine the variation in groundwater levels between 1930 and 2018. Groundwater levels are calculated by

subtracting the rest water level (rwl) from the surface elevation. Rest water level refers to the depth of water in a borehole measured from the ground surface. A deforming unit's maximum groundwater level for any given year is determined by the maximum level of groundwater within that area. Moreover, we analyze the relationship between groundwater abstraction and land subsidence by examining the temporal trend of groundwater level estimates. Despite the fact that the two datasets do not overlap in time, the spatial variation in groundwater level change may suggest a link between subsiding regions and groundwater abstraction. In addition, the borehole data is superimposed on the InSAR velocity estimate map in order to examine the relationship between subsiding regions and borehole density distribution. Due to the mismatch between the groundwater level and InSAR velocity estimates, we conducted a correlation analysis using groundwater levels for 2015–2018.

3 Results

3.1 Land subsidence patterns and rates for the period 2007–2010

SBAS processing of ALOS data reveals that there are multiple locations that have experienced land subsidence, as shown in Fig. 3. Despite their spatial distribution, most subsiding areas are located in built-up areas and follow the same linear direction in the southwest-northeast direction. One of the sites with the highest subsidence rates is an industrial site northeast of Nairobi (point f), where it occurs at a rate of approximately 47 mm/yr. There are also significant subsiding regions at the Ngara-Eestleigh estates (point c) off the Moi airbase airport (point c) at a rate of 30 mm/yr, Kibera (point a') at a rate of 35 mm/yr, Westlands (point b) at a rate of 14 mm/yr, and Mathare North estate (point i) at a rate of 17 mm/yr. On the basis of their spatial extents, subsiding regions can be regarded as localized deformations.

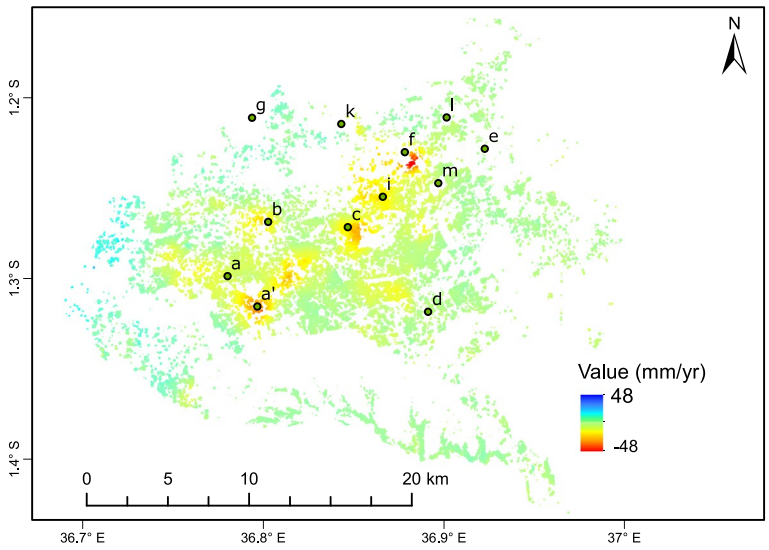

Fig. 3 LOS velocity estimates for the years 2007–2010 based on ALOS processing. In the map, the points indicate areas where significant subsidence has been observed during the periods of observation 2007–2010 and 2017–2021

3.2 Land subsidence patterns and rates for the period 2017–2021

In both ascending and descending Sentinel-1 processing, multiple areas with significant land subsidence were identified with similar spatial patterns and magnitudes. Furthermore, as shown in Fig. 4, velocity estimates are strongly correlated between the two orbits. The area (region aa') west of Nairobi exhibits the highest rate of subsidence, at a rate of approximately 48 mm/year in the direction of satellite line of sight as shown in Fig. 5. A total of 2000 ha fall under the region covered by points (aa') with the most extensive subsidence, which includes parts of Langata, Kibera, and Dagoreti North constituencies. This region has more extensive land subsidence than other places that have subsidence. There are other areas with significant land subsidence such as Mathare North extending into Garden Estate (region ijk), Westlands near Consolata shrine extending into parklands (point b), Ngara-Eastleigh estates off Moi Airbase airport point (point c), Kasarani estate extending into Roysambu (points ei), Fourways Junction Mall (point k), Ruaka near Two Rivers Mall (point g), and at the edges of Dandora landfill (point m).

The majority of subsiding locations are located in Nairobi's northern and western areas, as was true for ALOS processing results. However, we observe one isolated location (point d) in a residential area east of Nairobi as shown in Fig. 5

3.3 A comparison of velocity estimates for 2007–2010 and 2017–2021

On the basis of two observation periods, mixed results can be seen in terms of spatial patterns and subsidence rates. In each of the two observation periods, subsidence was observed in Westlands (point b), Ngara (point c), and Kibera-upper hill (region aa').

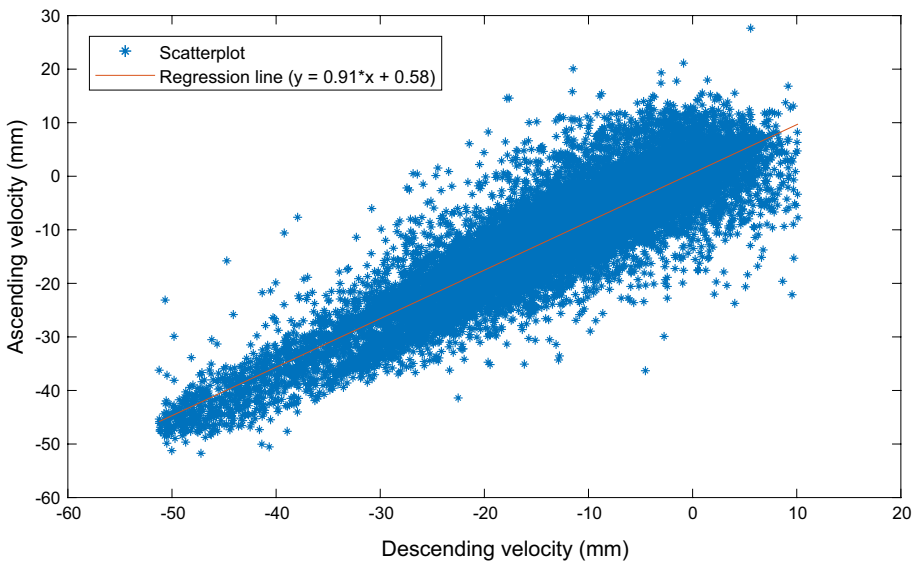

Fig. 4 A scatter plot displaying the correlation between Sentinel-1 ascending orbit and descending orbit velocity estimates for the period 2017–2021

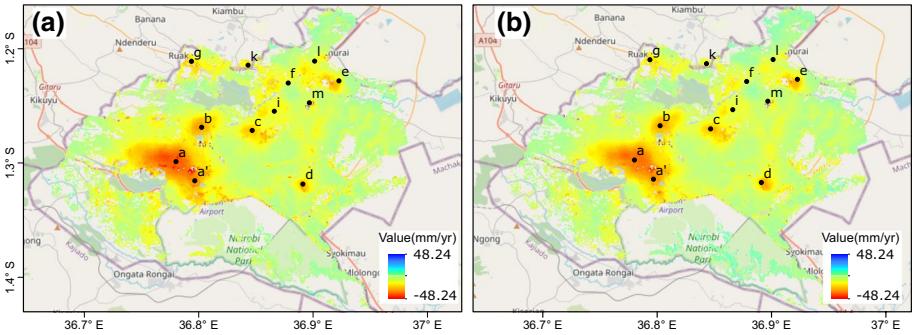

Fig. 5 A comparison of Sentinel-1 LOS velocity estimates for ascending (**a**) and descending (**b**) orbits clipped to the footprint of ascending track

Moreover, both the spatial extent as well as the magnitude of these subsiding locations have increased. One example of this growth can be seen in the spatial extent of the two subsiding areas (b and aa'). The two subsiding regions could merge if they experience the same subsidence rate. As well, there are new areas with high subsidence rates that were not recorded during the 2007-2010 period, including Embakasi near pipeline estate (point d), Kasarani (point e), and Ruaka (point g). Another noteworthy observation is the point f in Fig. 3 , which is located within East African Breweries Limited (EABL). It suffered significant subsidence between 2007 and 2010, but it incurred insignificant subsidence between 2017 and 2021. Except for point f, it can be observed that the average subsidence rate has risen at all other locations, as shown in Table 1. It should be noted, however, that for the period 2007-2010, the SBAS network was not as robust as the Sentinel-1 SBAS network due to a limited number of ALOS images. Still, the two datasets demonstrate consistent spatial patterns of land subsidence, supporting the claim that the locations have significantly subsided.

It should be noted that there is a seven-year gap between the two observations. In order to understand land subsidence during the period between two observations, we used a 3-year Sentinel-1 interferogram, as shown in Fig. 6. The interferogram was unwrapped

Table 1 LOS velocity estimates between 2007–2010 and 2017–2021 for selected points

Point	2007–2010	2017–2021
a	−5.79	−47.79
b	−9.41	−31.29
c	−11.62	−27.1
d	1.2	−22.76
e	−0.87	−32.48
f	−46.63	5.95
g	–	−26.5
i	−14.24	−17.02
j	−13.08	−19.06
k	4.01	−17.37
l	−15.08	−22.47
m	−4.72	−30.97

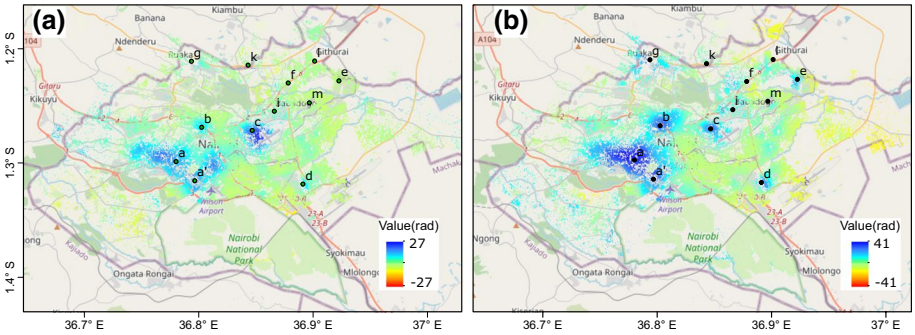

Fig. 6 Evolution of the land subsidence as measured by Sentinel-1 descending orbit over a three-year period between 2014–2017 and 2017–2020. (**a**) shows unwrapped interferograms from 2014-11-04 to 2017-02-09, whereas (**b**) shows unwrapped interferograms from 2017-02-09 to 2020-12-20. Note for interferogram a positive value implies movement away from the satellite

with an unwrapping factor of 0.3. Due to the urban nature of the study region and the orbital tube of Sentinel-1, the coherence of most parts remains high even for longer baseline intervals as shown in Appendix C. The subsidence areas in the MTI analysis matched those in the interferogram. A comparison of the two interferograms provides information about the evolution of the new places that have experienced land subsidence since 2010. As in MTI processing results regions aa', b and c also subsided between 2014 and 2020. Nevertheless, it can be observed that region c experienced the most subsidence between 2014 and 2017 compared to region b, which experienced higher subsidence rates between 2017 and 2020. Subsidence began in region D between 2014 and 2017 compared to the other locations that started subsiding after 2010. However, in some areas, such as locations e, g, i, k, and m, subsidence has been documented since 2017.

3.4 Time series displacement and direction of land subsidence

By combining the ascending and descending data, the velocity estimates of the vertical and east-west components indicate that subsidence occurs primarily in the vertical direction as shown in Fig. 7. A significant degree of lateral deformation does not appear to exist. The estimates are well within the range of the accuracy of LOS estimates, without showing any particular pattern. Apart from some locations within region aa' that recorded the highest subsidence rates, which may have been a result of the intense subsidence observed in this region.

Figure 8 shows a time-series plot that indicates how displacement rates have changed over time for selected points. It is evident from the time-series displacement estimates that most places are linearly displaced. For instance, location point a was observed to show linear displacement during both observation intervals, though higher subsidence rates were observed during the 2017-2021 observation period. Some sites, however, that have recently subsided or have ceased subsiding, have also shown a different temporal pattern. As an example, Location point f, which experienced significant subsidence between 2007 and 2010, stabilized between 2017 and 2021. For the two locations (points d and e) where subsidence was not detected during 2007–2010, the time series displacement estimates are in agreement with the interferogram results. As can be seen, location point d began

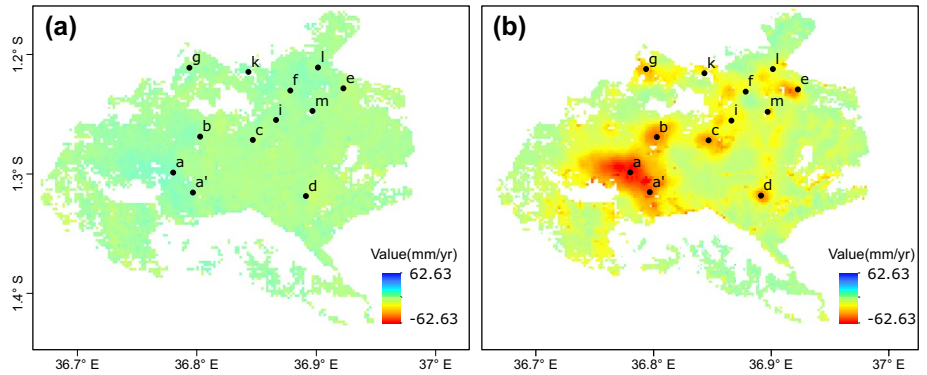

Fig. 7 Comparison of horizontal (east-west) and vertical components of velocity. (**a**) shows the horizontal component, whereas (**b**) shows the vertical component. We disregard the north-south component due to the lower sensitivity of the InSAR in this direction

subsiding toward the end of 2010 and has continued to subside continuously since that time. In contrast, location point e began subsiding at the beginning of the year 2019.

4 Discussion

4.1 Groundwater exploitation as a driver of subsidence

It is noteworthy that almost all the regions where subsidence has occurred also have experienced a significant decline in groundwater levels. For example, the groundwater levels in region a with the highest subsidence rate declined by approximately 100 meters between 2000 and 2018, which is the largest decline within the city, as shown in Fig. 9. This region has the highest number and density of boreholes, characterized by a decrease in the water table as compared to other places within Nairobi County, as noted by Nato (2015) and Ochungo et al. (2019). It has been reported that the water table in this region drops by 7 meters per year as opposed to the 3 meters in other regions (Chakava et al. 2014). A marked decline in groundwater levels has also been observed in the boreholes in regions b and c. The subsidence detected in these regions may be linked to overexploitation of groundwater. The groundwater table in region d has not changed significantly based on borehole data only available between 2010 and 2015.

Previous hydrogeological studies predicted that there is a possibility of land subsidence in Nairobi as a result of overexploitation of groundwater. As an example, the sites mentioned by Mathu et al. (2014), while difficult to evaluate since the data is not spatially presented, coincide with regions where land subsidence is occurring. Furthermore, EABL (point f) installed a water recycling plant towards the end of 2007, which dramatically reduced the water demand (Wakhungu et al. 2017; EABL 2011). Hence, this may explain why no subsidence has been observed between 2017 and 2021. The most common areas for subsidence are in residential areas, since most landowners supplement their piped water with borehole water. Thus the subsidence observed in some residential estates, such as Kasarani (point e), can also be attributed to ground water overexploitation. Despite the fact that we do not have borehole data

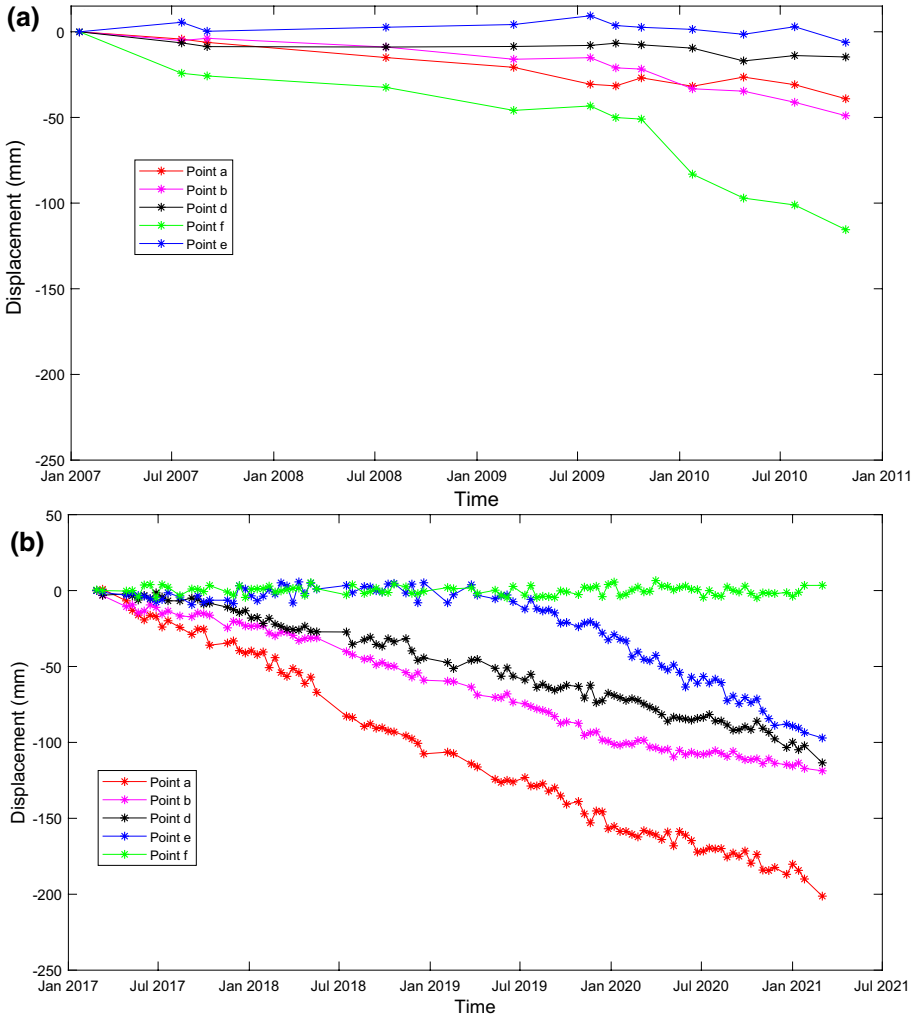

Fig. 8 Time series displacement estimates for selected points for the time periods 2007–2010 (**a**) and 2017–2021 (**b**). The map in Fig. 3 shows the location of each of the points

at this location, we believe subsidence is caused by overexploitation of groundwater, given the general trend of new buildings to supplement piped water with groundwater. Additionally, an analysis of the time series of displacement rates indicates a linear trend without any seasonal variation, which confirms that the subsidence is primarily caused by inelastic settlement, which is consistent with hydrogeological modelling performed by Mathu et al. (2014).

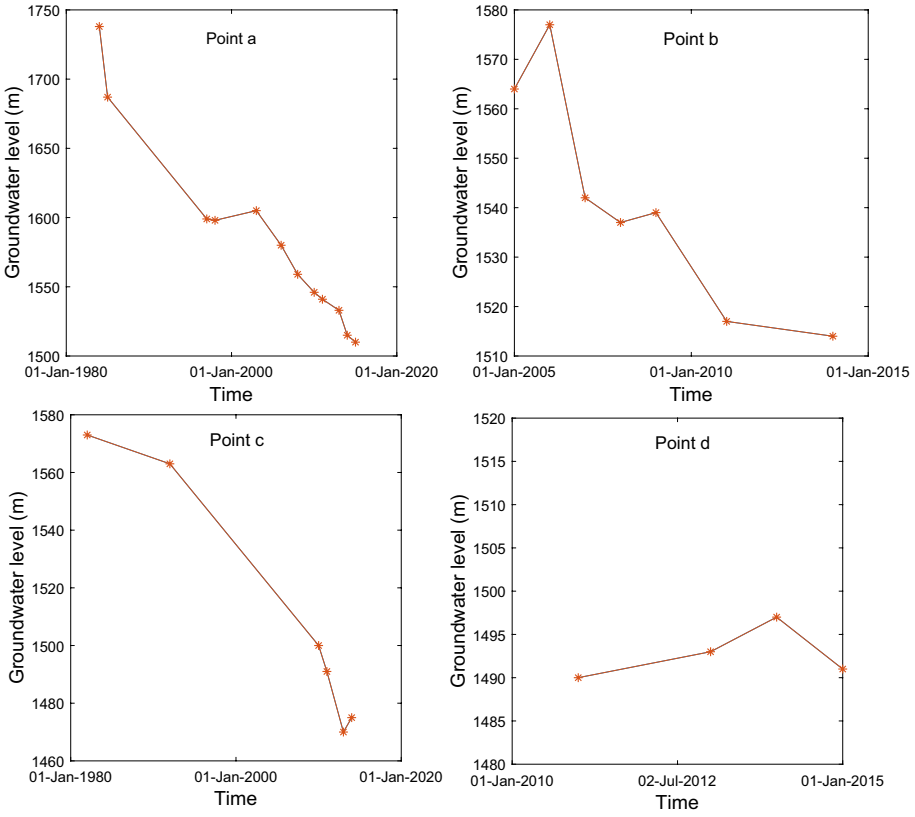

Fig. 9 An illustration of how groundwater levels have changed over time at sites that have experienced significant subsidence

4.2 Other causative agents

In Nairobi, there is also land subsidence that is unrelated to the overexploitation of underground water. For example, Kibera (point a') noted to have subsided in both observation periods is located within the floodplain of the Ngong River. It is the largest informal settlement in Kenya, with an estimated population of 300,000 people (Ndemo 2020; Ren et al. 2020). The area had been a marsh before the settlement (Ngugi et al. 2012) and is known to flood (Mulligan et al. 2016). It appears that subsidence at this location is the result of consolidation associated with the construction of unplanned structures on the floodplain, as illustrated in Fig. 10. Due to the types of structures and the level of poverty in the neighborhood, it is unlikely that subsidence is caused by overexploitation of underground water.

The area east of Nairobi has an unfavorable geomorphology, which does not facilitate the presence of high-yield groundwater (Onyango 2018). This might account for the low spatial distribution of boreholes in the area. In view of this, the isolated localized subsidence at Embakasi (location d) cannot be attributed solely to overexploitation of groundwater. In this particular case, the subsidence is attributed to consolidation, which occurs because of the loading effect of the buildings. This location has a dense population

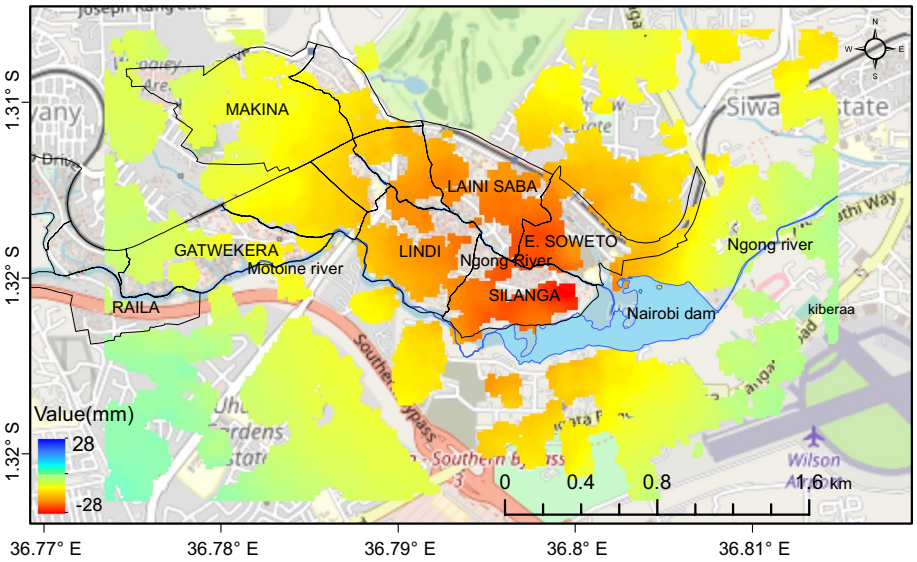

Fig. 10 Location of Kibera in relation to the Ngong and Mutoine rivers overlayed with Sentinel-1 velocity maps illustrating land subsidence in Kibera

of residential units comprising high-rise buildings with a large number of tenants (Mwau 2019).

According to the time-series displacements, the region did not subside during the period of 2007–2010. High-rise buildings constructed after 2007 have led to subsidence due to consolidation, as illustrated in Fig. 11, the area of subsidence is limited, and the adjacent residential areas are not subsiding. The results of this study coincide with those of other studies reporting localized subsidence associated with higher building densities (Xu et al. 2012; Yang et al. 2018).

Dandora Landfill subsidence as illustrated in Fig. 12 is caused both by consolidation and by biochemical processes within the landfill. The landfill itself does not show signs of subsidence due to the low coherence of the surface, which is caused by the constantly changing surface properties of the dumpsite as it is still in use. Similar findings have been made in other parts of the world, such as at Nanjido landfill (Baek et al. 2019), where it is possible that the continued disposal of the waste could endanger the structures within the landfill and the neighboring properties.

In the northwest of Nairobi, recent development on previously undeveloped land has caused subsidence. The growth of the Two Rivers Mall and the subsequent developments of the surrounding neighborhood may be attributed to subsidence at (location g). Subsidence is seen at two airports (Wilson and Moi Airbase) and is described as a result of foundation settlement caused by the consolidation of filling material during construction as well as the loading effect during takeoff and landing. Subsidence due to the takeoff and landing of planes has been reported in other cities (Aobpaet et al. 2013; Mesri and Funk 2015; Gao et al. 2016). It is worth noting, however, that the two airports are located off two subsiding regions, aa' and c, and the observed land subsidence can also be explained by adjacent deformation. A precise deformation monitoring system, although currently lacking, could provide important insights into the subsidence of these two airports.

Fig. 11 The evolution of residential buildings in Embakasi pipeline estate (point d) in Fig. 7. The image on the left illustrates the distribution of residential units before 2010 while the image on the right illustrates the current distribution. The red outline illustrates the extends of the current land subsidence. The images were taken from Google Earth

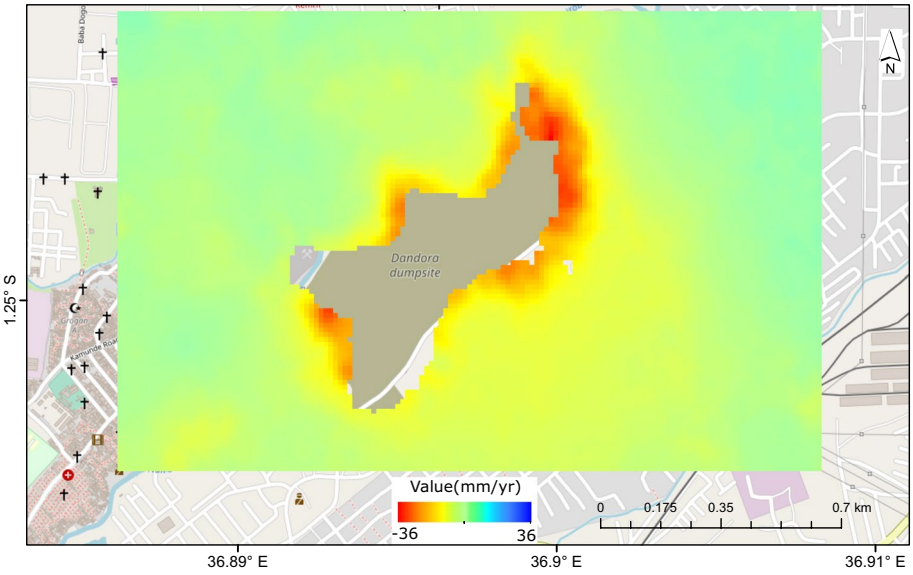

Fig. 12 Sentinel-1 velocity map illustrating land subsidence around the Dandora landfill

4.3 Implications of the observed land subsidence

The Nairobi water and sewerage company operates an extensive sewer network covering most of the city. The drainage system relies on gradient flow in order to drain sewage into the sewerage system's main trunk. The cumulative displacement of approximately 30 cm over the past five years has the potential to negatively affect the structural integrity of the existing sewer system. This may result in drainage backflow or flooding. In recent years, Nairobi has experienced periodic flooding that has been attributed to poor drainage caused by clogs in the sewer system as well as blocks in natural drainage paths (Baariu et al. 2017). Interestingly, there was significant subsidence in flooding-prone areas such

as in South C and Ngara . It is therefore probable that flooding in these regions is also a consequence of land subsidence, which alters the slope of the drainage system as a result of uneven subsidence of the land. Additionally, flooding in the informal settlements of Kibera can be attributed to the modification of floodplains as a result of land subsidence. In the process of designing flood mitigation measures for Nairobi County, it is critical to take into account the impact of land subsidence.

The lack of an updated geodetic network suggests that vertical geodetic control over subsiding areas is inherently unreliable. Thus, it is imperative that engineering projects within Nairobi County relying on geodetic control be aware of significant land subsidence and incorporate these effects into their design. In the case of subsidence, it is possible, for example, that road construction projects that cross subsiding areas could create drainage problems. It is because a displacement in vertical direction of over 100 cm in a section of road can cause drainage problems. In the same way, the observed cracks in the buildings may be due to land subsidence. An investigation conducted by the Building Directorate of Kenya in 2016 found that 7 percent of buildings in Nairobi West with region aa' exhibited signs of cracking (Kenya Engineer 2016). The cracks are frequently attributed to structural problems, but due to the intense subsidence in this area, they may also be related to subsidence. There is also the possibility that the number could be higher since the owners of these buildings tend to conceal cracks on their walls from authorities out of fear that their buildings will be condemned. The observed land subsidence therefore necessitates the updating of the geodetic network and the development of a dynamic geodetic network capable of incorporating the anticipated rate of subsidence.

Nairobi's land subsidence characterization is an invaluable tool that can be used by various sectors of the economy to guide policy discussions and future decisions. For instance, it is possible that the water resource authority may use this tool among other things to regulate the issuance of drilling permits for boreholes, and to zone areas where groundwater extraction is no longer feasible. Nairobi County government may use the land subsidence map to update spatial plans and prepare mitigation plans, while small property owners and banks should be informed of the potential destruction of buildings caused by land subsidence, which impacts the valuation of those properties. Despite the fact that the direct effects of land subsidence have yet to be documented, intense flooding and the depletion of aquifers are clear indicators of subsidence. Due to the importance of Nairobi, it is important that measures be taken to mitigate the effects of recorded subsidence.

5 Conclusion

Our findings empirically agree with those of previous hydrological studies that have suggested land subsidence in Nairobi. Our study quantified land subsidence spatially, identifying regions with substantial subsidence. Land subsidence is mostly concentrated in the built-up areas in the western and northwestern parts of Nairobi. Although land subsidence occurred gradually at most locations, we observed the emergence of new locations with significant subsidence. Land subsidence occurs linearly in the vertical direction, with the highest velocity recorded west of Nairobi at a rate of approximately 60 mm/year. There is an overlap between regions with a higher decline in groundwater levels and areas with intense land subsidence, along with linear displacement in the vertical direction. This suggests the main cause of land subsidence is the exploitation of groundwater. Land subsidence in other parts, however, is due to factors such as

consolidation due to the loading of buildings and landfill, changes in land use due to rapid urbanization, and development along the Ngong River floodplain. The interplay of these factors has led to the rapid expansion of regions with significant land subsidence in previously stable areas, such as the land subsidence observed in the east and northwest of Nairobi. The increased availability of data and improved processing algorithms has facilitated deformation monitoring in regions that were not previously possible because of the costs involved in setting and maintaining the geodetic network. With the identification of regions with significant subsidence, InSAR can be used to allocate limited resources by designing a geodetic deformation-monitoring system to capture subsidence at sites that have already been identified. Hence, future research will focus on utilizing InSAR results to design a deformation monitoring network for Nairobi County and guide the location of observation wells, which could provide reliable borehole data with good temporal resolution and information, such as pumping and recharge rates.

Appendix

Appendix A

SBAS network for ascending and descending orbit for Sentinel-1 data. The ascending network contains 497 interferograms, while the ascending network contains 402 interferograms.

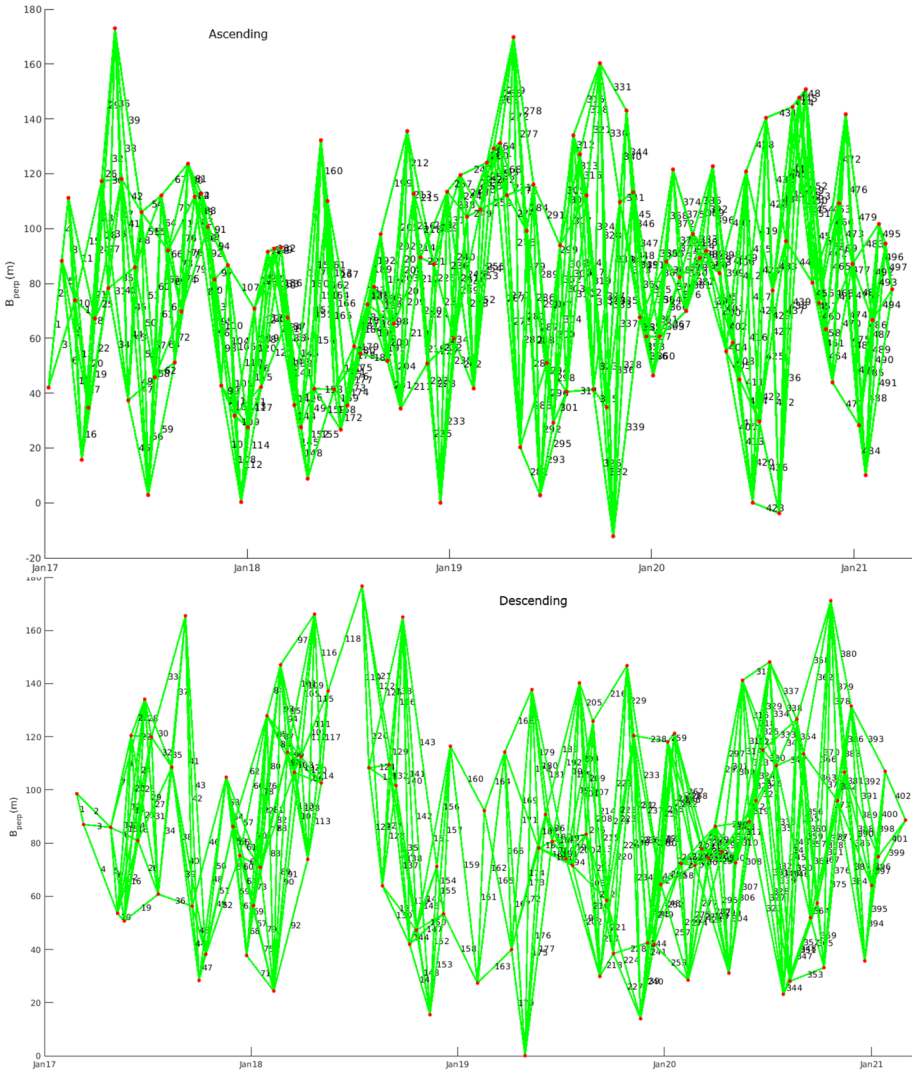

Appendix B

ALOS SBAS network. The dots represent the SAR images, while the lines represent the interferograms. There are 49 interferograms in the network.

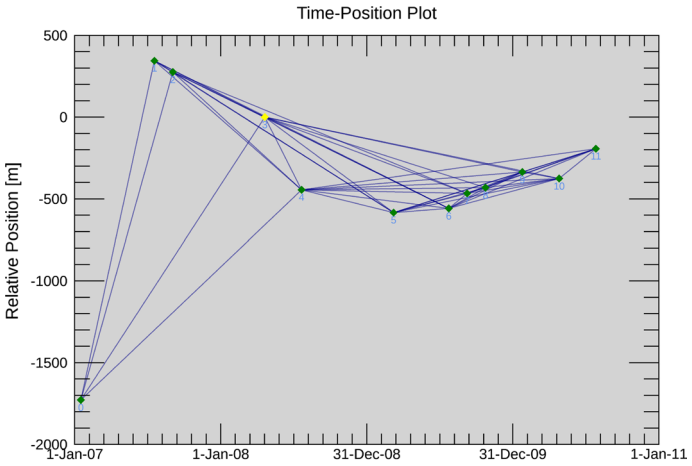

Appendix C

The coherence map corresponding to the Interferogram 2014–2017 as shown in the Fig. 6.

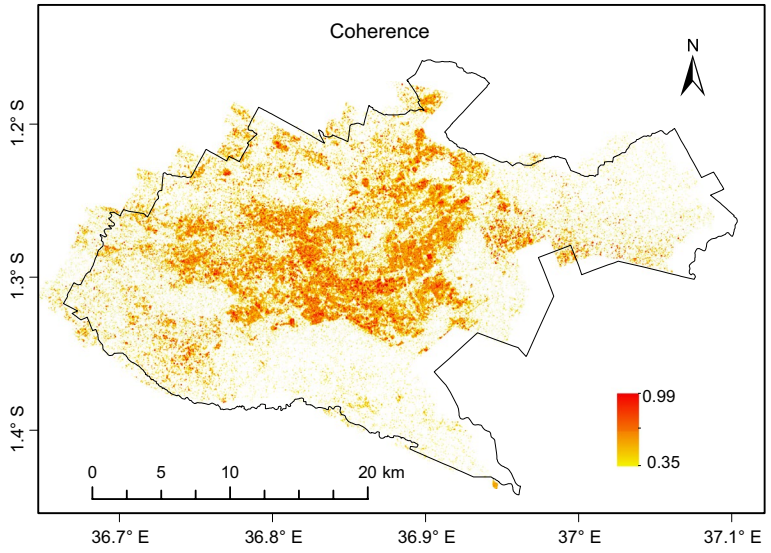

Acknowledgements This work was funded by the Kenya-Germany postgraduate training programme administered by the DAAD. We would like to thank the Kenya Water Resources Agency for the borehole data and the European Space Agency (ESA) for providing the SAR images. In all figures, the base maps are taken from Open Street Maps (© OpenStreetMap contributors). Additionally, we would like to thank Geofrey Gichuru for his assistance during the ground truthing process. Furthermore, we wish to thank the two reviewers for their invaluable comments, which helped to improve the manuscript.

Funding Open Access funding enabled and organized by Projekt DEAL.

Declarations

Conflict of interest The authors declare that they have no conflict of interest.

References

Abidin HZ, Andreas H, Gumilar I, Fukuda Y, Pohan YE, Deguchi T (2011) Land subsidence of Jakarta (Indonesia) and its relation with urban development. Nat Hazards 59(3):1753

Aobpaet A, Cuenca MC, Hooper A, Trisirisatayawong I (2013) InSAR time-series analysis of land subsidence in Bangkok, Thailand. Int J Remote Sens 34(8):2969–2982

Argyrakis P, Ganas A, Valkaniotis S, Tsioumas V, Sagias N, Psiloglou B (2020) Anthropogenically induced subsidence in Thessaly, central Greece: new evidence from GNSS data. Nat Hazards 102(1):179–200

Baariu P et al (2017) Assessment of flood management in south c ward of nairobi city county, Kenya. PhD thesis, University of Nairobi

Baek WK, Jung HS, Jo MJ, Lee WJ, Zhang L (2019) Ground subsidence observation of solid waste landfill park using multi-temporal radar interferometry. Int J Urban Sci 23(3):406–421

Berardino P, Fornaro G, Lanari R, Sansosti E (2002) A new algorithm for surface deformation monitoring based on small baseline differential SAR interferograms. IEEE Trans Geosci Remote Sens 40(11):2375–2383

Bhattarai R, Alifu H, Maitiniyazi A, Kondoh A (2017) Detection of land subsidence in Kathmandu Valley, Nepal, using DInSAR technique. Land 6(2):39

Chakava Y, Franceys R, Parker A (2014) Private boreholes for Nairobi's urban poor: The stop-gap or the solution? Habitat Int 43:108–116

Chaussard E, Wdowinski S, Cabral-Cano E, Amelung F (2014) Land subsidence in central Mexico detected by ALOS InSAR time-series. Remote Sens Environ 140:94–106

Chen B, Gong H, Li X, Lei K, Ke Y, Duan G, Zhou C (2015) Spatial correlation between land subsidence and urbanization in Beijing, China. Nat Hazards 75(3):2637–2652

Chen C, Pei S, Jiao J (2003) Land subsidence caused by groundwater exploitation in Suzhou City, China. Hydrogeol J 11(2):275–287

Chrzanowski A, Yong-qi C, Leeman RW, Leal J, Maraven (1989) Integration of the global positioning system with geodetic leveling surveys in ground subsidence studies. CISM J 43(4):377–386

de Luna RMR, dos Anjos Garnés SJ, Cabral JJdSP, dos Santos SM (2017) Groundwater overexploitation and soil subsidence monitoring on Recife plain (Brazil). Nat Hazards 86(3):1363–1376

EABL (2011) Eabl annual report and financial statements 2011. Tech rep, URL https://africanfinancials.com/document/ke-eabl-2011-ar-00/

Eriksen HØ, Lauknes TR, Larsen Y, Corner GD, Bergh SG, Dehls J, Kierulf HP (2017) Visualizing and interpreting surface displacement patterns on unstable slopes using multi-geometry satellite SAR interferometry (2D InSAR). Remote Sens Environ 191:297–312

Ezquerro P, Del Soldato M, Solari L, Tomás R, Raspini F, Ceccatelli M, Fernández-Merodo JA, Casagli N, Herrera G (2020) Vulnerability assessment of buildings due to land subsidence using InSAR data in the ancient historical city of Pistoia (Italy). Sensors 20(10):2749

Fattahi H, Agram P, Simons M (2016) A network-based enhanced spectral diversity approach for TOPS time-series analysis. IEEE Trans Geosci Remote Sens 55(2):777–786
Ferretti A, Prati C, Rocca F (2000) Nonlinear subsidence rate estimation using permanent scatterers in differential SAR interferometry. IEEE Trans Geosci Remote Sens 38(5):2202–2212
Foster S, Tuinhof A (2005) The role of groundwater in the water supply of greater Nairobi, Kenya. World Bank Case Profile Collection 13
Gao M, Gong H, Chen B, Zhou C, Chen W, Liang Y, Shi M, Si Y (2016) InSAR time-series investigation of long-term ground displacement at Beijing Capital International Airport, China. Tectonophysics 691:271–281
Gasperini D, Allemand P, Delacourt C, Grandjean P (2014) Potential and limitation of uav for monitoring subsidence in municipal landfills. Int J Environ Technol Manage 17(1):1–13
Geudtner D, Torres R, Snoeij P, Davidson M, Rommen B (2014) Sentinel-1 system capabilities and applications. In: 2014 IEEE Geoscience and Remote Sensing Symposium, IEEE, pp 1457–1460
Goldstein RM, Werner CL (1998) Radar interferogram filtering for geophysical applications. Geophys Res Lett 25(21):4035–4038
Guo H, Zhang Z, Cheng G, Li W, Li T, Jiao JJ (2015) Groundwater-derived land subsidence in the north china plain. Environ Earth Sci 74(2):1415–1427
Guth A, Wood J (2013) Geological map of the southern kenya rift. Digital Map and Chart Series DMCH016 Geological Society of America
Haghighi MH, Motagh M (2019) Ground surface response to continuous compaction of aquifer system in tehran, iran: results from a long-term multi-sensor insar analysis. Remote Sens Environ 221:534–550
Haregu TN, Ziraba AK, Aboderin I, Amugsi D, Muindi K, Mberu B (2017) An assessment of the evolution of kenya's solid waste management policies and their implementation in nairobi and mombasa: analysis of policies and practices. Environ Urban 29(2):515–532
Hirose K, Maruyama Y, Murdohardono D, Effendi A, Abidin HZ (2001) Land subsidence detection using JERS-1 SAR Interferometry. In: 22nd Asian Conference on Remote Sensing, pp 5–9
Hooper A (2008) A multi-temporal insar method incorporating both persistent scatterer and small baseline approaches. Geophys Res Lett 35(16)
Hooper A, Zebker HA (2007) Phase unwrapping in three dimensions with application to insar time series. JOSA A 24(9):2737–2747
Hooper A, Bekaert D, Spaans K, Arıkan M (2012) Recent advances in sar interferometry time series analysis for measuring crustal deformation. Tectonophysics 514:1–13
Hu J, Li ZW, Ding XL, Zhu JJ, Zhang L, Sun Q (2014) Resolving three-dimensional surface displacements from InSAR measurements: a review. Earth Sci Rev 133:1–17
Hudson Hill S (2020) A terrible beauty: art and learning in the anthropocene. J Museum Educ 45(1):74–90
Kenya Engineer (2016) Technical audit of buildings as a tool for disaster risk reduction. URL https://www.kenyaengineer.co.ke/technical-audit-of-buildings-as-a-tool-for-disaster-risk-reduction/
KNBS (2019) Population and Housing Census Report. Tech. rep., URL https://housingfinanceafrica.org/documents/2019-kenya-population-and-housing-census-reports/
Makunda CS (2018) Sustainable housing through sustainable planning practices: Challenges and opportunities for formal housing provision in nairobi, kenya. In: Lifelong learning and education in healthy and sustainable cities, Springer, pp 539–549
Matheson FJ (1966) Geology of the Kajiado area. Geological Survey of Kenya Report 70
Mathu EM, Onyancha C, Mwea S, Ngecu W (2014) Effects of drilling deep tube wells in the urban areas of Nairobi city, Kenya
Measurement Systems Limited (2018) Muya CORS. URL https://muya-cors.com/
Mesri G, Funk JR (2015) Settlement of the Kansai international airport islands. J Geotech Geoenviron Eng 141(2):4014102
Motagh M, Shamshiri R, Haghighi MH, Wetzel HU, Akbari B, Nahavandchi H, Roessner S, Arabi S (2017) Quantifying groundwater exploitation induced subsidence in the rafsanjan plain, southeastern iran, using insar time-series and in situ measurements. Eng Geol 218:134–151
Mulligan J, Harper J, Kipkemboi P, Ngobi B, Collins A (2016) Community-responsive adaptation to flooding in kibera, kenya. In: Proceedings of the institution of civil engineers-engineering sustainability, Thomas Telford Ltd, 170:268–280
Mumma A, Lane M, Kairu E, Tuinhof A, Hirji R (2011) Kenya groundwater governance case study
Mwau B (2019) The rise of nairobi's concrete tenement jungle. URL https://goodmenproject.com/social-justice-2/the-rise-of-nairobis-concrete-tenement-jungle/

Mwaura OK, Odera PA (2021) Monitoring spatio-temporal compliance of urban development plans using gis and remote sensing in nairobi city county, kenya. Ghana J Geography 13(3)
Nairobi City Council (2007) City of Nairobi Environment Outlook. Tech. rep
Nato S (2015) Groundwater Management Practice in Nairobi County
Ndemo B (2020) Slum digitisation, its opponents and allies in developing smart cities: The case of kibera, nairobi. In: Open Cities| Open Data, Springer, pp 129–148
Neelmeijer J, Schöne T, Dill R, Klemann V, Motagh M (2018) Ground deformations around the Toktogul reservoir, Kyrgyzstan, from envisat ASAR and sentinel-1 data-A case study about the impact of atmospheric corrections on InSAR time series. Remote Sens 10(3):1–21. https://doi.org/10.3390/rs10030462
Ngugi E, Benoit C, Hallgrimsdottir H, Jansson M, Roth EA (2012) Partners and clients of female sex workers in an informal urban settlement in Nairobi, Kenya. Cult Health Sexual 14(1):17–30
NWSC (2019) Status of water supply to the city. URL https://www.nairobiwater.co.ke/wp-content/uploads/2021/03/STATUS_OF_WATER_SUPPLY_PRESS_RELEASE_1.pdf
Ochungo EA, Ouma GO, Obiero JPO, Odero NA (2019) An assessment of groundwater grab syndrome in Langata Sub County, Nairobi City-Kenya. J Water Resour Prot 11(05):651
Oiro S, Comte JC, Soulsby C, MacDonald A, Mwakamba C (2020) Depletion of groundwater resources under rapid urbanisation in Africa: recent and future trends in the Nairobi Aquifer System, Kenya. Hydrogeol J 28(8):2635–2656. https://doi.org/10.1007/s10040-020-02236-5
Onyancha C, Dalyot S, Siriba D, Sester M (2012) Modelling of spatial and temporal variations in groundwater rest levels in Nairobi City using geographic information system. Nile Water Sci Eng J 5(1):26–33
Onyancha CK, Mathu EM, Mwea SK, Ngecu WM (2011) Dealing with sensitive and variable soils in Nairobi city. 9:282–291
Onyango MO (2018) Modelling the effects of urban morphology on environmental quality of Nairobi city, Kenya. PhD thesis, University of Eldoret
Otiso KM, Owusu G (2008) Comparative urbanization in ghana and kenya in time and space. GeoJournal 71(2–3):143–157
Pratesi F, Tapete D, Del Ventisette C, Moretti S (2016) Mapping interactions between geology, subsurface resource exploitation and urban development in transforming cities using InSAR Persistent Scatterers: Two decades of change in Florence, Italy. Appl Geogr 77:20–37
Prats-Iraola P, Scheiber R, Marotti L, Wollstadt S, Reigber A (2012) TOPS Interferometry With TerraSAR-X. IEEE Trans Geosci Remote Sens 50(8):3179–3188. https://doi.org/10.1109/TGRS.2011.2178247
Rateb A, Abotalib AZ (2020) Inferencing the land subsidence in the nile delta using sentinel-1 satellites and gps between 2015 and 2019. Sci Total Environ 729:138868
Ren H, Guo W, Zhang Z, Kisovi LM, Das P (2020) Population density and spatial patterns of informal settlements in Nairobi, Kenya. Sustainability 12(18):7717
Sahraoui OH, Hassaine B, Serief C, Hasni K (2006) Radar interferometry with sarscape software. Photogrammetry and Remote Sensing
Sandwell DT, Myer D, Mellors R, Shimada M, Brooks B, Foster J (2008) Accuracy and resolution of alos interferometry: vector deformation maps of the father's day intrusion at Kilauea. IEEE Trans Geosci Remote Sens 46(11):3524–3534
Stamps DS, Nyblade A, Kianji G (2019) Uganda-Kenya Eastern Branch GNSS Network - KYN2. The GAGE Facility operated by UNAVCO, Inc., GPS/GNSS Observations Dataset. https://doi.org/10.7283/879W-ZH24
Tosi L, Teatini P, Carbognin L, Frankenfield J (2007) A new project to monitor land subsidence in the northern Venice coastland (Italy). Environ Geol 52(5):889–898
Ustun A, Tusat E, Yalvac S (2010) Preliminary results of land subsidence monitoring project in Konya Closed Basin between 2006–2009 by means of GNSS observations. Nat Hazard 10(6):1151–1157
Wakhungu M, et al. (2017) A cost benefit analysis of water recycling in manufacturing industries: a case study of the east african breweries limited, Kenya. PhD thesis, University of Nairobi
Xu YS, Ma L, Du YJ, Shen SL (2012) Analysis of urbanisation-induced land subsidence in Shanghai. Nat Hazards 63(2):1255–1267
Yang Q, Ke Y, Zhang D, Chen B, Gong H, Lv M, Zhu L, Li X (2018) Multi-scale analysis of the relationship between land subsidence and buildings: a case study in an eastern Beijing urban area using the PS-InSAR technique. Remote Sens 10(7):1006